Cancer Chemother Pharmacol (2011) 68:619–629
DOI 10.1007/s00280-010-1521-8

ORIGINAL ARTICLE

Cytochrome P450 ω-hydroxylase promotes angiogenesis and metastasis by upregulation of VEGF and MMP-9 in non-small cell lung cancer

Wei Yu · Li Chen · Yu-Qing Yang · John R. Falck · Austin M. Guo · Ying Li · Jing Yang

Received: 20 June 2010 / Accepted: 3 November 2010 / Published online: 1 December 2010

Abstract
Purpose Cytochrome P450 (CYP) ω-hydroxylase, mainly consisting of CYP4A and CYP4F, converts arachidonic acid to 20-hydroxyeicosatetraenoic acid (20-HETE) that induces angiogenic responses in vivo and in vitro. The present study examined the role of CYP ω-hydroxylase in angiogenesis and metastasis of human non-small cell lung cancer (NSCLC).
Methods The effect of WIT003, a stable 20-HETE analog, on invasion was evaluated using a modified Boyden chamber in three NSCLC cell lines. A549 cells were transfected with CYP4A11 expression vector or exposed to CYP ω-hydroxylase inhibitor (HET0016) or 20-HETE antagonist (WIT002), and then ω-hydroxylation activity toward arachidonic acid and the levels of matrix metalloproteinases (MMPs) and VEGF were detected. The in vivo effects of CYP ω-hydroxylase were tested in established tumor xenografts and an experimental metastasis model in athymic mice.
Results Addition of WIT003 or overexpression of CYP4A11 with an associated increase in 20-HETE production significantly induced invasion and expression of VEGF and MMP-9. Treatment of A549 cells with HET0016 or WIT002 inhibited invasion with reduction in VEGF and MMP-9. The PI3 K or ERK inhibitors also attenuated expression of VEGF and MMP-9. Compared with control, CYP4A11 transfection significantly increased tumor weight, microvessel density (MVD), and lung metastasis by 2.5-fold, 2-fold, and 3-fold, respectively. In contrast, WIT002 or HET0016 decreased tumor volume, MVD, and spontaneous pulmonary metastasis occurrences.
Conclusion CYP ω-hydroxylase promotes tumor angiogenesis and metastasis by upregulation of VEGF and MMP-9 via PI3 K and ERK1/2 signaling in human NSCLC cells.

Keywords Cytochrome P450 · 20-HETE · Metastasis · Angiogenesis · NSCLC

Introduction

Non-small cell lung cancer (NSCLC) is the leading cause of cancer death worldwide. Most deaths still result from local and distant metastasis. About two-thirds of such recurrences are in distant organs, such as brain, contralateral lung, and bone as a result of the hematogenous spread of cancer cells. Multiple chemotherapy combinations have been studied, and no particular regimen has provided a significant improvement in outcomes [1]. Therefore, it is important to better understand the mechanisms involved in the spread of lung cancer and find more effective targets for improving the outcomes for patients.

Cytochrome P450 (CYP) ω-hydroxylase, mainly consisting of CYP4A and CYP4F, metabolizes arachidonic acid to

W. Yu · L. Chen · Y. Li · J. Yang (✉)
Department of Pharmacology, School of Medicine,
Wuhan University, Donghu Road, Wuhan 430071, China
e-mail: yangjingliu@yahoo.com.cn

Y.-Q. Yang
School of Pharmacy, China Pharmaceutical University,
Nanjing 210009, China

J. R. Falck
University of Texas Southwestern Medical Center,
Dallas, TX, USA

A. M. Guo
Department of Women's Health Services, Gynecologic Oncology,
Henry Ford Health System, Detroit, MI, USA

biologically active eicosanoids including 20-hydroxyeicosatetraenoic acid (20-HETE), which has numerous important physiological and pathological functions [2]. 20-HETE has been reported to serve as a second messenger in the mitogenic actions of a number of growth factors [3], and an important mediator of vascular endothelial growth factor (VEGF) mediated angiogenesis and vessel sprouting [4]. N-hydroxy-N-(4-butyl-2 methylphenyl)-formamidine (HET0016), a selective inhibitor of 20-HETE synthesis [5, 6], was found to inhibit the angiogenic responses to EGF, VEGF, FGF, and electrical stimulation in rats [7, 8] and block angiogenesis in the cornea stimulated by the implantation of human U251 glioblastoma cells as well as the proliferation of U251 cells in vitro [7, 9]. WIT002, an antagonist of 20-HETE, inhibited the growth of renal adenocarcinoma in nude mice [10], and the proliferation of U251 cells transfected with CYP4A1 in vitro [11]. In contrast, WIT003, a stable 20-HETE agonist, stimulated endothelial cell proliferation and VEGF expression in vitro [12]. These data suggest that CYP ω-hydroxylase may play an important role in tumor growth and angiogenesis. Interestingly, ω-hydroxylation activity toward arachidonic acid was high in the nuclear envelope fraction of A549 NSCLC cells [13]. However, there is no information available about the role of CYP ω-hydroxylase in angiogenesis and metastasis of NSCLC.

Growing evidence shows that lung cancer cells secrete high levels of growth factors and matrix-degrading proteases, including VEGF [14] and matrix metalloproteinases (MMPs) [15, 16], which are found to be significantly associated with survival in NSCLC patients [17, 18]. Many studies have documented that VEGF regulates most of the steps in the angiogenesis cascade and is a critical mediator of angiogenesis [19], and MMPs are able to release bound-VEGF and regulate most of the steps in the angiogenesis cascade [20]. Furthermore, MMP-9 has been associated with active neovascularization and tumor invasion because these MMPs can degrade the extracellular matrix, essential steps in the process of angiogenesis and metastasis [21–24]. Therefore, agents possessing the ability to suppress the activities and expression of VEGF and MMPs are worthy targets of development for anti-lung cancer angiogenesis and metastasis.

In this study, we investigated whether CYP ω-hydroxylase increases the angiogenic and metastatic potential of human NSCLC cells and found CYP ω-hydroxylase enhanced invasion in vitro as well as angiogenesis and metastasis in vivo and significantly increased the expression of VEGF and MMP-9 in vitro and in vivo. In addition, our results showed the importance of the PI3 K/Akt and ERK1/2 signaling pathway in these process. These observations suggest that CYP ω-hydroxylase may represent a worthy target for therapy of NSCLC.

Materials and methods

Chemicals

Antibodies against human VEGF and MMP-9 were purchased from Santa Cruz Biotechnology, Inc (Santa Cruz, CA). In addition, HET0016 and 20-HETE-d6 were purchased from Cayman Chemicals (Ann Arbor, MI). WIT003 [20-hydroxyeicosa-5(Z), 14(Z)-dienoic acid] and WIT002 [20-hydroxyeicosa-6(Z), 15(Z)-dienoic acid] were synthesized by one of the authors John R. Falck. Antibodies against PI3 K, Akt, JNK, ERK, and p38 (including phosphorylated forms) were purchased from Cell Signaling Technology (Beverly, MA). The specificity of polyclonal antibodies against human CYP4A11 was purchased from Research Diagnostics (Flanders, NJ). Anti CD-34 antibody was purchased from DAKO Corporation (Carpenteria, CA). MMP-2, MMP-9, VEGF ELISA Kit, and mouse anti-human VEGF monoclonal antibody were purchased from R&D Systems (Minneapolis, MN). The VEGFR2-receptor inhibitor SU5416 was provided by SUGEN (San Francisco, CA). All other compounds were purchased from Sigma Chemical Co (St. Louis, MO).

Cell cultures and transfection

Human NSCLC cell lines A549, H1299, and SW-1573 were obtained from ATCC. Cells were grown according to the manufacturer's recommendations and maintained at 37°C in a humidified incubator containing 5% CO_2. Human CYP4A11 complementary DNA (cDNA) was obtained by RT-PCR of the RNA prepared from hepatocellular cells and subcloned into a pCI-neo expression GFP (Promega, Madison, WI). pCI-neo-GFP vector was previously described [25]. The plasmid including the CYP4A11 cDNA or the plasmid alone was transfected into A549 cells with a Transfast Transfection Reagent kit (Promega). Stable transformants were selected by 4 weeks' cultured in the presence of 600 μg/ml G418 and isolated by a single cell manipulation technique. Protein in established clones was studied. Cells were treated with vehicle (ethanol), WIT003, WIT002, HET0016, wortmannin, U0126, or left untreated, as indicated, for invasion or other studies.

In vitro cell invasion assays

In vitro cell invasion assays were performed in 10-mm-diameter and 8-μm pore polycarbonate filter transwell plates. Membranes were precoated with 25 μg of matrigel on the upper surface, which formed a reconstituted basement membrane at 37°C. Cells were seeded onto the upper well of the chamber. Subsequently, serum-free medium with HET0016 (10 μmol/L), WIT002(10 μmol/L), WIT003

(0.01, 0.1, 1 μmol/L), or ethanol as a control was added to the upper chamber, while the lower well was filled to the top (500 μL) with RPMI-1640 containing 5% fetal calf serum (FCS) as a chemoattractant. Cells were allowed to migrate for 5 h. The non-migrating cells were then carefully removed from the upper surface of the transwell with a wet cotton swab, and cells were fixed for 30 min in 4% formaldehyde and stained for 15 min with crystal violet. Cells that had invaded to the bottom surface of the filter were counted with an ocular micrometer in a blinded manner, counting a minimum of 10 high-powered fields (HPF).

Murine xenograft model of tumor growth and metastasis

All animal studies were approved by the Animal Research Committee of Wuhan University and maintained in accordance with Association for Assessment and Accreditation of Laboratory Animal Care (AAALAC). Athymic BALB/c mice, 6–8 weeks of age, were provided by the Experimental Animal Center of Wuhan University and were housed on a 12-h light/12-h dark cycle in a pathogen-free environment and allowed ad libitum access to food and water. A549-CYP4A11 or A549-GFP cells (5×10^6) were injected subcutaneously (s.c.) into the flank of nude mice. After 2 days, the mice were subcutaneously injected HET0016 (10 mg/kg), WIT002 (10 mg/kg) or 10% lecithin in water as a control once per day. The mice were examined for localized tumor, and the tumor size was measured once every three days (beginning 7 days after injection) with microcalipers. Tumor volume was measured with a digital caliper and calculated using the formula $0.52 \times a \times b^2$, wherein a and b are the largest and smallest diameters as described previously [26]. The mice were euthanized 6 weeks after the inoculation. The weight of each tumor was measured. Xenograft tumors were sectioned and stained using anti-CD34 antibodies. The areas of invasive tumor containing the highest numbers of capillaries and small venules per area (''hotspots'') were selected by light microscopy at low magnification (×100). After the area of the highest neovascularization was identified, individual microvessel counts were blindly made on a 400× field. Results were expressed as the mean value of all the fields.

The implantation of A549-CYP4A11 cells into the lung was done as previously described [27]. Briefly, the left chest of each anesthetized mouse was incised (5-mm incision) just below the inferior border of the scapula, then 20 μL of suspension containing 1×10^6 cells and 20 μg of matrigel were injected into the left lung parenchyma through the intercostal space. The skin incision was closed with 3–0 silk. After 2 days, the mice were treated with or without HET0016 (10 mg/kg) and WIT002 (10 mg/kg) once per day by subcutaneously injection. Mice were euthanized 30 days after tumor cell implantation. Tumors were examined in lung, mediastinal lymph node, liver, kidney, and spleen and were weighed.

Measurement of CYP arachidonic acid ω-hydroxylation activity

20-HETE, the major CYP ω-hydroxylase metabolite of arachidonic acid, was analyzed by liquid chromatography mass spectrometry (LC/MS/MS) as previously described [8, 28]. In brief, tissue and cells were collected and homogenized in 1 ml of a 0.1 M KPO_4 buffer containing 5 mM $MgCl_2$ and 1 mM EDTA. The homogenate was incubated for 30 min at 37°C with a saturating concentration of arachidonic acid (40 μM) and 1 mM NADPH in the presence and absence of 10 μM HET0016. The reaction was stopped by acidification with formic acid to pH 3.5 and extracted twice with 3 vols of ethyl acetate after the addition of 2 ng of an internal standard 20-HETE-d6. The organic phase was dried under nitrogen. Mass spectrometric analysis was performed on an Agilent LSD ion trap mass spectrometer 1100 (Agilent Technologies) using negative electrospray ionization-MS/MS, and the peaks eluting with a mass/charge ratio (m/z) of 319 (20-HETE) or 326.5 (20-HETE-d6) were isolated and monitored. The ratio of ion abundance in the peaks of interest (20-HETE; m/z 319) versus that corresponding to the closely eluting internal standard (20-HETE-d6; m/z 326.5) was determined.

ELISA analysis

ELISA assay for VEGF, MMP-2, and MMP-9. A549 cells with various treatments were seeded in six-well plates. After 24 h, the cells were incubated with serum-free medium for another 24 h and then treated with HET0016, WIT002, or ethanol as a control in 1% FBS for 24 h. The culture media and tumor homogenate were collected, centrifuged to remove cellular debris, and stored at −70°C until assay for VEGF, MMP-2, and MMP-9. The cells in the plate were trypsanized, and the total number of cells was determined by cell counting. The assay was done using a commercially available VEGF, MMP-2, and MMP-9 ELISA kit according to the manufacturer's instructions. For MMP-2 and MMP-9 assay, the culture media (500 μL) were concentrated using the microcon concentrator (Millipore). Results were normalized to the cell number.

Analysis of MMP-2 and MMP-9 activities

The activities of MMP-2 and MMP-9 were assayed by gelatin zymography as described previously [29]. Briefly, samples containing equal amounts of protein were subjected to 10% SDS–polyacrylamide gel containing 0.1% gelatin. Electrophoresis was performed at 80 and 120 V for

3 h. Gels were then washed twice in zymography washing buffer (2.5% Triton X-100 in double-distilled H_2O) at room temperature to remove SDS, followed by incubation at 37°C for 12–16 h in zymography reaction buffer (40 mM Tris–HCl (pH 8.0), 10 mM $CaCl_2$, 0.02% NaN_3), stained with Coomassie blue R-250 (0.125% Comassie blue R-250, 0.1% amino black, 50% methanol, 10% acetic acid) for 1 h and destained with destaining solution (20% methanol, 10% acetic acid, 70% double-distilled H_2O). Non-staining bands representing the levels of the latent form of MMP-2 and MMP-9 were quantified by densitometer measurement using a digital imaging analysis system.

Western blotting analysis

Proteins were extracted from xenograft tumors or cells for immunoblot analysis. Protein concentration was determined by Bradford method, and 20 μg of protein extract was subjected to electrophoresis in 8% polyacrylamide slab gels and transferred to PVDF membrane, blocked with 5% nonfat milk, and probed with PI3 K, Akt, ERK, JNK, p38 (including phosphorylated forms), CYP4A11, CYP4F2, VEGF, and MMP-9 antibodies. Blots were washed, incubated with a peroxidase-conjugated antibody, and chemiluminescence detection was performed using an enhanced chemiluminescence kit according to the manufacture's protocol.

Statistical analysis

All values are expressed as mean ± SEM, and statistical analyses were performed using one-way ANOVA followed by the Student-Newman-Keul's test. Values were compared using for multiple comparisons, where P values of 0.05 or less were considered significant.

Results

CYP ω-hydroxylase stimulates invasion in H1299, SW-1573, and A549 cells

It has been reported that WIT003 and 20-HETE have similar angiogenenic responses in endothelial cells, and WIT003 cannot be metabolized by cyclooxygenase enzymes to prostanoids due to lack of double bonds in the 11, 12 and 8, 9 positions [12]. Therefore, a parallel experiment was conducted to confirm the equivalency of WIT003 with 20-HETE on invasion under identical conditions in three NSCLC cell lines. We found that H1299, SW-1573, and A549 cells treated with WIT003 at doses of 0.01–1 μM increased invasion (onefold to threefold increase over control; Fig. 1a). Our results also showed that 20-HETE induced a similar and comparable dose-dependent increase in invasion compared with WIT003 (data not shown). Because there was no significant difference between the effects of 20-HETE and WIT003, we chose to use WIT003 for most subsequent experiments.

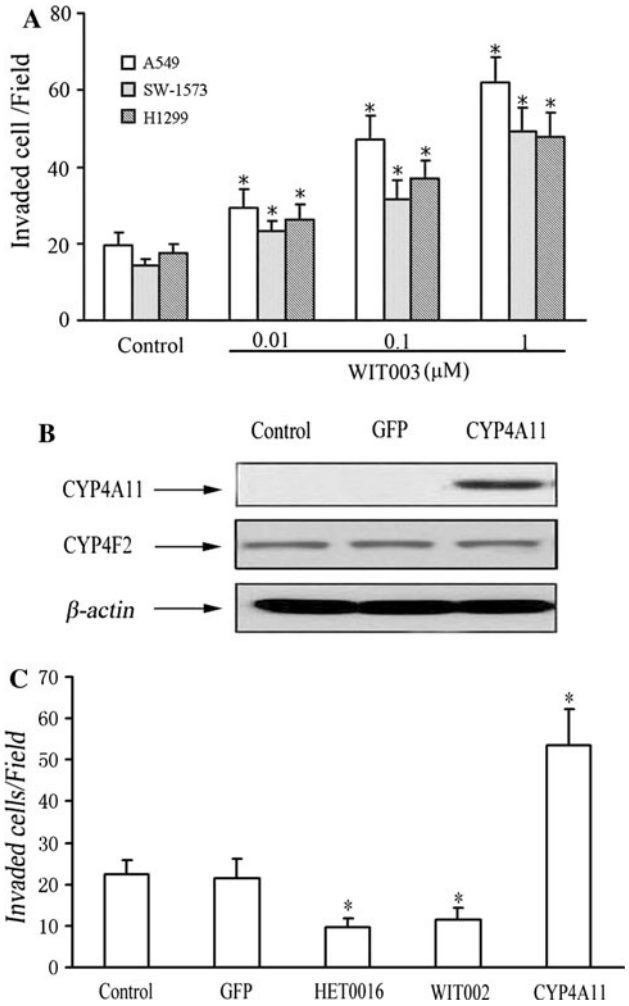

Fig. 1 CYP ω-hydroxylase overexpression or WIT003 promotes invasion in NSCLC cells. **a** H1299, SW-1573, and A549 cells were treated with various concentrations of WIT003 (0.01, 0.1, and 1 μmol/L each), and cell invasion was also measured in a 5-h transwell assay in a blinded manner. **b** Expression of CYP4A11 and CYP4F2 in A549 cells or 1 wk after transfection with CYP4A11. **c** Cell invasion was measured from A549 cells treated with WIT002, HET0016 or transfected with CYP4 A11 in a 5-h transwell assay. $^{*}P < 0.05$, $^{**}P < 0.01$ versus control group; Representative data are shown as mean ± SEM from a single experiment ($n = 6$)

It is documented that the expression of CYP4A11 mRNA in A549 cells was not detected [13], and CYP4A11 has the advantage of being a potent 20-HETE synthase while having negligible ability to form epoxides [12]. Thus, we transfected the CYP4A11 cDNA to A549 cells and found that CYP4A11 transfection resulted in increased expression of the respective recombinant proteins compared with cells transfected with GFP or untransfected cells

(Fig. 1b). And then, the effect of CYP4 A11 overexpression on invasion of A549 cells was assessed in vitro using transwell assay and found it increased the invasion to twofold compared with control. Moreover, ω-hydroxylation activity toward arachidonic acid was high in A549 cells [13]; thus, A549 cells were treated with HET0016 or WIT002 in the invasion assays, and we found both of them significantly decreased invasion (Fig. 1c). Together, these results indicate that CYP ω-hydroxylase enhances invasion of NSCLC cells in vitro.

CYP ω-hydroxylase enhanced subcutaneous tumor size and angiogenesis

Having shown the role of CYP ω-hydroxylase in NSCLC cell invasion, we went on to evaluate its tumor growth and angiogenesis properties using tumor models xenografted in athymic mice. Mice injected with A549-CYP4 A11 cells showed significantly enhanced tumor growth rate (Fig. 2a) and size (Fig. 2b) compared with control. In contrast, tumors in mice treated with HET0016 or WIT002 grew slower and smaller. In addition, A549-CYP4A11 tumors appeared earlier (6.9 ± 3.2 days) than control, and tumor originating from A549 cells treated with HET0016 or WIT002 appeared later (16.2 ± 2.5 days; 15.3 ± 2.6 days;) than control (10.5 ± 2.5 days) and GFP group (11.4 ± 3.4 days; $P < 0.05$). At 6 weeks, all animals were euthanized, and no metastatic tumor was observed in any organs.

Capillary vessel counting in and around primary tumors showed that CYP4A11 transfection significantly increased microvessel density (MVD) (34.1 ± 7.3/HPF in control and 35.32 ± 6.4/HPF in GFP group vs. 63.8 ± 11.4/HPF in A549-CYP4A11 group, $P < 0.05$). In contrast, both HET0016 and WIT002 significantly decreased MVD compared with control group (16.3 ± 4.6/HPF in HET0016 group and 21.3 ± 5.1/HPF in WIT002 group versus control, $P < 0.05$; Fig. 2c). These results suggest that CYP ω-hydroxylase-derived 20-HETE enhances tumor growth and angiogenesis for primary tumors.

CYP ω-hydroxylase enhanced experimental lung metastasis of A549 cells in nude mice

In the experimental metastasis model, CYP4A11 overexpression also led to significantly more lung metastases than control (Fig. 2d). A549-CYP4A11 and A549-GFP groups formed local tumors in the lung in five of six and four of six nude mice, respectively, 30 days after transplantation. Metastatic tumors from A549-CYP4A11 groups were observed in mediastinal lymph nodes in five of six mice with lung tumors at 6 weeks, and two animals had liver metastatic lesions (7 and 9 metastatic foci, respectively). The mean tumor number in A549-CYP4A11 groups was significantly more than those of A549-GFP groups, and there were only two metastasis in mediastinal lymph nodes from the mouse with lung tumors of A549-GFP groups. In contrast, treatment with HET0016 or WIT002 significantly reduced the tumor incidence and mediastinal lymph node metastases compared with control, and there were no metastases to other organs. Together, these results indicate that CYP ω-hydroxylase-derived 20-HETE promotes tumor metastatic potential in vivo.

ω-Hydroxylation activity toward arachidonic acid in homogenates from A549 cell and A549 tumor

Given the arachidonic acid as substrate, we determined the concentration of its metabolite, 20-HETE. The levels of 20-HETE were significantly higher in A549-CYP4A11 cells (53.1 ± 8.6 pmol/min/mg protein in CYP4A11 groups vs. 21.2 ± 4.9 pmol/min/mg protein in control, $P < 0.01$; Fig. 3a) and A549-CYP4A11 tumor (48.3 ± 6.9 pmol/min/mg protein in A549-CYP4A11 groups vs. 26.3 ± 4.7 pmol/min/mg protein in control, $P < 0.05$; Fig. 3b). In contrast, the levels of 20-HETE were inhibited by HET0016 in A549 cells or A549 tumors homogenates. These data suggested that CYP4A11 overexpression markedly enhanced the ω-hydroxylation activity toward arachidonic acid, and HET0016 is able to inhibit the activities of CYP ω-hydroxylase in A549 cells.

CYP ω-hydroxylase induced expression of VEGF and MMP-9

Angiogenesis and metastasis are associated with expression of various molecules, including VEGF and MMPs. The effect of CYP ω-hydroxylase on expression of these genes was examined in A549 cells and in excised tumor xenografts. We found that CYP4A11 overexpression up-regulated VEGF and MMP-9 at the levels of protein compared with control. Conversely, the VEGF and MMP-9 levels were decreased by HET0016 or WIT002 treatment. In addition, CYP4A11 overexpression significantly up-regulated the MMP-9 activities compared with control, but it did not have any significant effects on the activity of MMP-2 (Fig. 4a, b, d). Together, these data suggested that CYP4A11-derived 20-HETE significantly up-regulated expression of the genes that promote angiogenesis and metastasis. To further determine whether 20-HETE-induced MMP-9 expression is mediated by VEGF, the effects of anti-VEGF or SU5416 on MMP-9 were measured in A549 cells or A549-CYP4A11 cells, and we found those treatments could partly abolish MMP-9 expression (Fig. 4c).

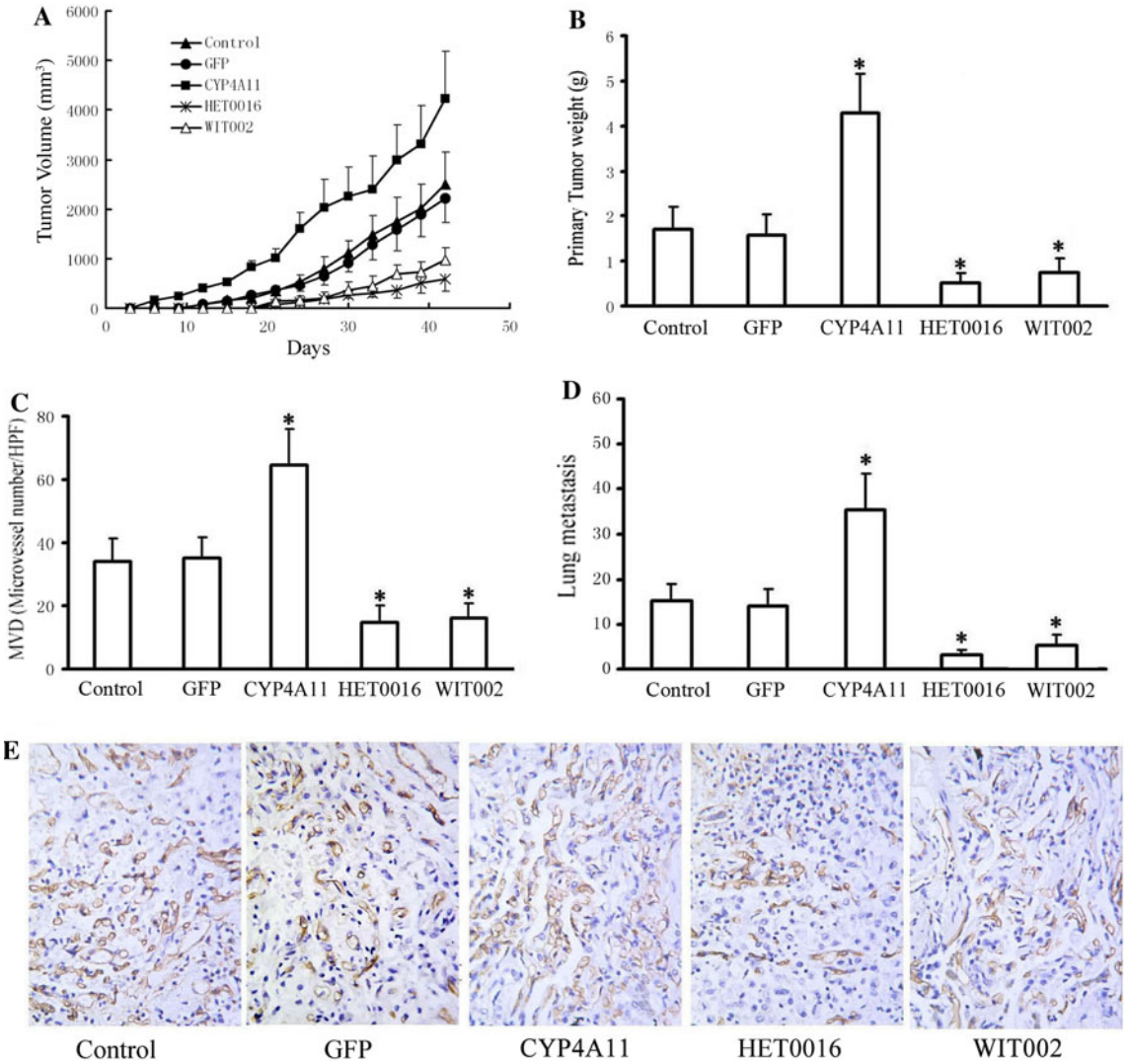

Fig. 2 CYP ω-hydroxylase in A549 cells promotes primary tumor growth, angiogenesis and metastasis to lungs in nude mice. Nude mice injected with A549 cells untransfected (control) or transfected CYP4A11 (A549-CYP4A11). After 2 days, the mice were treated with or without HET0016 (10 mg/kg) or WIT002 (10 mg/kg). **a** Primary xenograft tumor volume growth curves. **b** Average primary tumor weight for each group after growth for 6 weeks. **c** Average microvessel density in primary tumors and around tumors were counted in a blinded manner (MVD; capillary vessel number per HPF). **d** Average number of lung metastases for each group in experimental metastasis model. **e** Representative photographs of the tumor sections examined by immunohistochemical staining for CD34 (×400 magnification). $^{*}P < 0.05$, $^{**}P < 0.01$ versus control group ($n = 6$)

CYP ω-hydroxylase up-regulated VEGF and MMP-9 through PI3 K and ERK1/2 signaling pathways

Since we have shown CYP ω-hydroxylase induced expression of VEGF and MMP-9, the underlying mechanisms were further investigated. We investigated whether CYP ω-hydroxylase could affect the activation of MAPK and PI3 K/Akt signaling cascades in A549 cells. And the results showed CYP4A11 significantly induced the activation of ERK1/2 and PI3 K/Akt as shown by increasing the phosphorylation of ERK1/2 and PI3 K/Akt without affecting phospho-JNK1/2 and phospho-p38 activity. In contrast, treatment of A549 cells with WIT002 or HET0016 significantly decreased the phosphorylation of ERK1/2 and PI3 K/Akt (Fig. 5).To further confirm whether the effects of CYP ω-hydroxylase mainly occurred through the induction of the ERK1/2 or PI3 K/Akt signaling pathway, A549 cells were pretreated with a PI3 K inhibitor (wortmannin; 10 μM) or ERK inhibitor (U0126; 20 μM) for 1 h and then incubated in the present or absence of WIT003 (1 μM) for 24 h. In this study, we chose 1 μM WIT003 as our working concentration because the expression levels of VEGF and MMP-9 were increased concentration dependently by WIT003 at the dose of 0.01 ~ 1 μM (data not shown). We found that treatment of A549 cells with

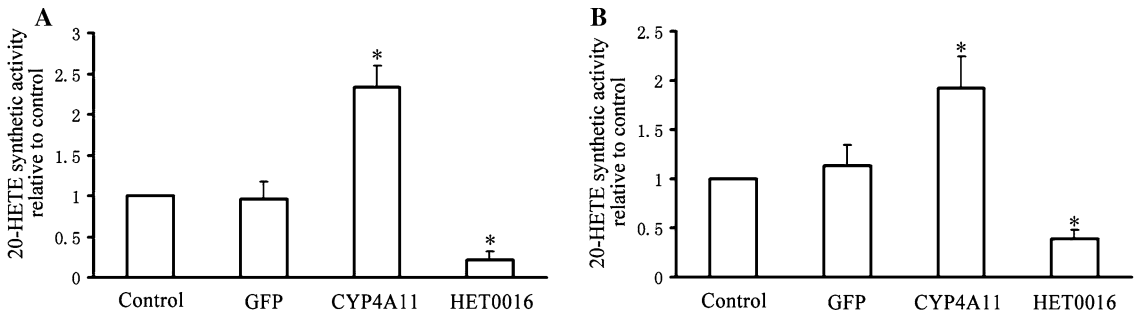

Fig. 3 Measurement of CYP arachidonic acid ω-hydroxylation activity. **a** 20-HETE synthesis was detected after incubation of A549 cell or A549-CYP4A11 cell extracts with arachidonic acid in the presence and absence of 10 μM HET0016. **b** 20-HETE synthesis was detected after incubation of A549 or A549-CYP4A11 tumor extracts with arachidonic acid in the presence and absence of 10 μM HET0016 in nude mice. $^{*}P < 0.05$ versus control group ($n = 6$)

these inhibitors markedly abrogated WIT003-induced VEGF and MMP-9 expression (Fig. 5c). Our data indicated the induction of the VEGF and MMP-9 expression by CYP ω-hydroxylase could occur through ERK1/2 and Akt activation.

Discussion

In the present study, we have provided direct evidence that WIT003 treatment markedly enhanced the invasion in three different NSCLC cell lines, and CYP4A11-transfection with an associated increase in 20-HETE production promoted angiogenesis and metastasis by upregulating expression of VEGF and MMP-9. In addition, we showed that HET0016 or WIT002 treatment profoundly inhibited invasion in vitro and angiogenesis and metastasis in vivo and significantly decreased the expression of VEGF and MMP-9 in vitro and in vivo. Furthermore, we have demonstrated that activation of PI3 K/Akt and ERK1/2 plays an important role in the upregulation of VEGF and MMP-9 afforded by CYP ω-hydroxylase (Fig. 6). Therefore, CYP ω-hydroxylase might be a new potential target for therapy of human NSCLC.

The development of metastases is a complex process composed of a cascade of linked, sequential, and highly selective steps including survival of tumor cells in the blood circulation, arrest in the capillary bed of the secondary organ, invasion into the secondary organ interstitium and parenchyma, proliferation, and induction of angiogenesis [30]. The metastatic propensity of a tumor may be influenced by the angiogenic potential of the tumor cells by two independent mechanisms: high microvessel density in the primary tumor may enhance the opportunity of tumor cells to gain access to the blood circulation, and elevated capacity to induce neovascularization may increase the probability of tumor cells trapped in secondary organ capillary beds to give rise to macroscopic tumor growth [31]. Our data show that the angiogenesis and metastasis potential of CYP ω-hydroxylase is indicated by the observed increase in incidence, weight, capillary vessel, and mediastinal lymph node metastases of tumors in the nude mice model. In vitro and in vivo, we have also shown that the mechanism by which CYP ω-hydroxylase promotes tumor cell invasion is through the upregulation of VEGF and MMP-9. It is demonstrated that VEGF are able to induce the expression of MMP-9 in the process of angiogenesis [32]. In our experiments, the effect of anti-VEGF and SU5416 on MMP-9 expression was also measured in A549 and A549-CYP4A11 cells, and the results indicated that MMP-9 expression, while directly induced by endogenous 20-HETE, was partly mediated by VEGF. Furthermore, MMP-9 is induced in clusters of premetastatic lung endothelial cells through VEGF receptor 1 (VEGFR1) signaling from distant primary tumors [33], indicating that MMP-9 and VEGF generated around tumors or in the peripheral circulation may facilitate the recruitment of VEGFR-1-positive hematopoietic stem and progenitor cells. Therefore, further experiments are being carried out to investigate this possibility.

It has been reported that HET0016, a selective inhibitor of 20-HETE synthesis, suppressed human U251 and 9L glioma cell proliferation in vitro and in vivo, and the effects seemed to be independent of 20-HETE synthesis inhibition [9, 34]. HET0016 and WIT002 markedly inhibit renal adenocarcinoma cell proliferation though decreased production or functional antagonism of 20-HETE [10]. This discrepancy could be due to differences of histological types of tumors (renal adenocarcinoma cell versus glioma cell). In this study, we investigated the role of CYP ω-hydroxylase in NSCLC cell lines and found that HET0016 or WIT002 potently inhibited the cell invasion, tumor growth, MVD, and metastasis. Given that high ω-hydroxylation activity toward arachidonic acid was likely due to CYP4F2, and there is no

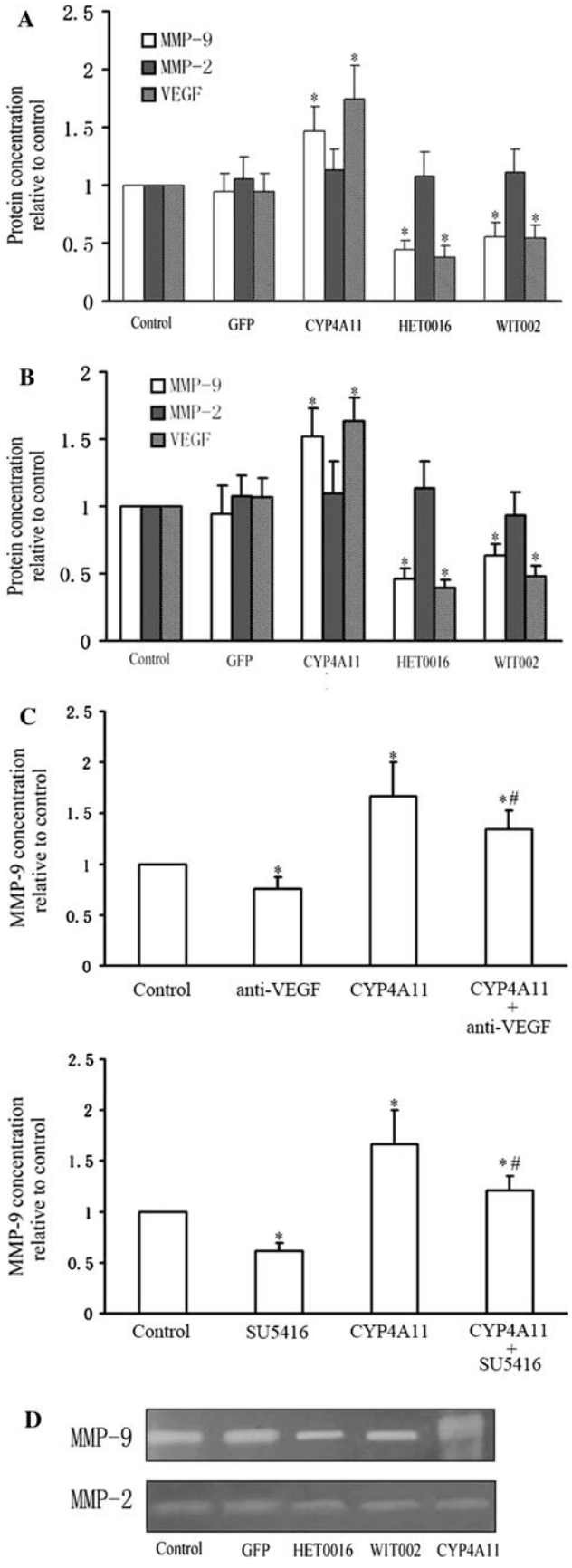

◀ **Fig. 4** CYP ω-hydroxylase influence activity and expression of VEGF and MMP-9 in A549 cells and xenograft tumors. **a** VEGF, MMP-2, and MMP-9 expression from A549 cells were treated with vehicle, WIT002, HET0016 or transfected with CYP4A11 for 24 h. $^{*}P < 0.05$, versus control group; **b** VEGF, MMP-2, and MMP-9 protein expression from A549-CYP4A11 tumor xenografts were treated with vehicle, HET0016 or WIT002 for 6 weeks. $^{*}P < 0.05$, versus control group; **c** MMP-9 protein expression from A549-CYP4A11 cells treated with anti-VEGF and SU5416 for 24 h. $^{*}P < 0.05$, versus control group; $^{\#}P < 0.05$, versus A549-CYP4A11; **d** Activities for MMP-2 and MMP-9 from A549 cells treated with HET0016, WIT002 or transfected with CYP4A11 for 24 h was analyzed using gelatin zymography. Representative data are shown as mean ± SEM from a single experiment ($n = 6$)

detectable amount of CYP4A11 and CYP4B1 mRNA in A549 cells [13, 35], the antiangiogenic and antimetastatic potential of HET0016 and WIT002 could be due to inhibition of CYP4F2 in A549 cells. In addition, altered CYP ω-hydroxylase activity or antagonised 20-HETE profoundly affected VEGF and MMP-9 in vitro and in vivo, suggested that 20-HETE-induced angiogenic and metastatic potential could be mediated by VEGF and MMP-9. Collectively, our results demonstrated that CYP ω-hydroxylase-derived 20-HETE promotes tumor angiogenesis and metastasis by upregulation of VEGF and MMP-9, and HET0016 and WIT002 have potent antiangiogenic and antimetastatic activities, suggesting their potential use in the treatment of human NSCLC.

PI3 K/Akt and MAPK signaling pathways are considered to be critical to regular proliferation, invasion, angiogenesis, and metastasis ability [36–38]. Recently, CYP ω-hydroxylase-derived-20-HETE is involved in activation of ERK1/2 and PI3 K/Akt in endothelial cells, suggesting that MAPK and PI3 K activation may be common pathways whereby high 20-HETE might influence endothelial cell function, such as proliferation [12] and apoptosis [39]. In addition, expression of CYP4A1-20-HETE alters cell growth in U251 human gliomas by a mechanism that initially involves activation of the ERK1/2 [11]. Our results showed CYP4A11 overexpression increased phospho-ERK1/2 and phospho-Akt in A549 cells and HET0016 or WIT002 inhibited endogenous 20-HETE stimulation of ERK1/2 and PI3 K/Akt. Furthermore, inhibitors for ERK1/2 (U0126) and PI3 K/Akt (wortmannin) suppressed WIT003-induced VEGF and MMP-9 expression, suggesting that the induction of VEGF and MMP-9 by CYP ω-hydroxylase involves the PI3 K and ERK1/2 signaling pathway.

In conclusion, our findings suggest that CYP ω-hydroxylase, mainly consisting CYP4A and CYP4F, promotes angiogenesis and metastatic potential of human NSCLC cells through the upregulation of VEGF and MMP-9 expression. The induction of VEGF and MMP-9 by CYP

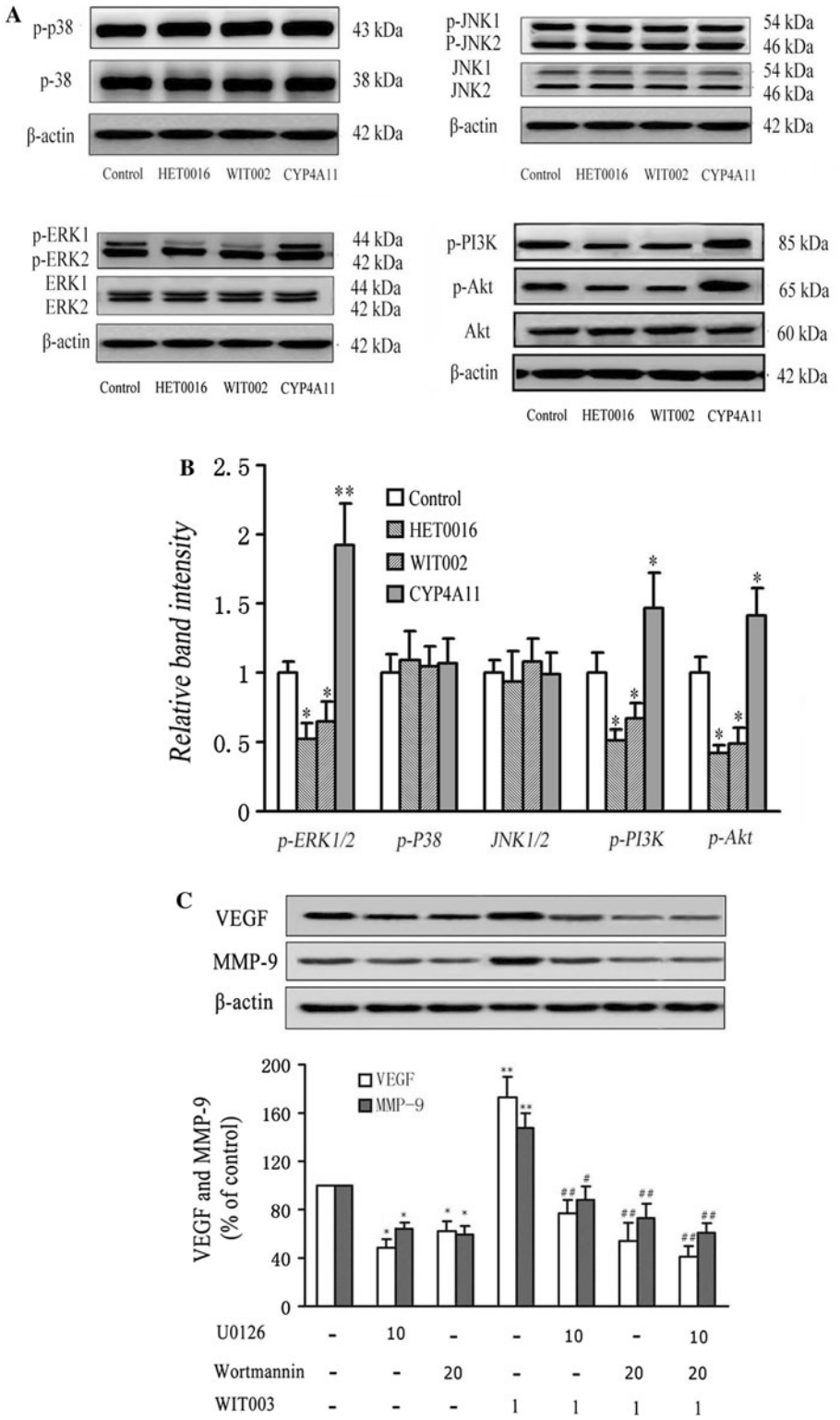

Fig. 5 Effect of CYP ω-hydroxylase activation of MAPK and PI3 K/Akt signaling. **a** Quantification of phospho-MAPKs and phosphor-PI3 K/Akt proteins was performed by densitometric analysis of the western blot. Cells were cultured in serum-free media in the absence or present of HET0016 or WIT002 for 12 h, and then the cell lysates were subjected to sodium dodecyl sulfate–polyacrylamide gel electrophoresis followed by western blots. **b** Effect of PI3 K inhibitor (wortmannin) and ERK inhibitor (U0126) on WIT003-induced the expression of VEGF and MMP-9. A549 cells were plated in six-well and pre-treated with wortmannin (10 μM) or U0126 (20 μM) for 1 h and then incubated for 24 h. Afterward, the culture medium was subjected to western blot to analyze the expression of VEGF and MMP-9. Protein determinations were subsequently quantified by densitometric analysis with that of control being 100% as shown just below the data. Each *bar* represents the mean ± SEM, $n = 6$, $^{*}P < 0.05$, $^{**}P < 0.01$ versus the control

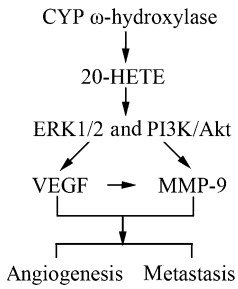

Fig. 6 The schematic presentation of our proposed mechanism of how CYP ω-hydroxylase promotes NSCLC cells angiogenesis and metastasis

ω-hydroxylase involves the PI3 K and ERK1/2 signaling pathway. Our findings should provide a clue for the development of novel therapeutic strategies and for the improved survival of patients with advanced lung cancer.

Acknowledgments We greatly thank Dr. Jiancheng Tu and Dr. Xie xianfei for their helpful discussions and reading of this manuscript. *Grant support*: National Nature Science Foundation Committee of China (No. 301162662), Science Foundation of Health Department of Hubei Province (No. JX3B14), National institutes of health Grant GM31278 (to J.R.F.), and the Robert A.Welch Foundation (to J.R.F.).

References

1. Granville CA, Dennis PA (2005) An overview of lung cancer genomics and proteomics. Am J Respir Cell Mol Biol 32:169
2. Miyata N, Roman RJ (2005) Role of 20-hydroxyeicosatetraenoic acid (20-HETE) in vascular system. J Smooth Muscle Res 41:175
3. Sun CW, Falck JR, Harder DR, Roman RJ (1999) Role of tyrosine kinase and PKC in the vasoconstrictor response to 20-HETE in renal arterioles. Hypertension 33:414
4. Stec DE, Gannon KP, Beaird JS, Drummond HA (2007) 20-Hydroxyeicosatetraenoic acid (20-HETE) stimulates migration of vascular smooth muscle cells. Cell Physiol Biochem 19:121
5. Miyata N, Taniguchi K, Seki T, Ishimoto T, Sato-Watanabe M, Yasuda Y, Doi M, Kametani S, Tomishima Y, Ueki T, Sato MKameo K (2001) HET0016, a potent and selective inhibitor of 20-HETE synthesizing enzyme. Br J Pharmacol 133:325
6. Seki T, Wang MH, Miyata N, Laniado-Schwartzman M (2005) Cytochrome P450 4A isoform inhibitory profile of N-hydroxy-N'-(4-butyl-2-methylphenyl)-formamidine (HET0016), a selective inhibitor of 20-HETE synthesis. Biol Pharm Bull 28:1651
7. Chen P, Guo M, Wygle D, Edwards PA, Falck JR, Roman RJScicli AG (2005) Inhibitors of cytochrome P450 4A suppress angiogenic responses. Am J Pathol 166:615
8. Sandra LA, Kristopher GM, Daniela NS, Richard JR, Andrew SG (2003) CYP4A metabolites of arachidonic acid and VEGF are mediators of skeletal muscle angiogenesis. Am J Physiol Heart Circ Physiol 284:1528
9. Guo M, Roman RJ, Falck JR, Edwards PAScicli AG (2005) Human U251 glioma cell proliferation is suppressed by HET0016 [N-hydroxy-N'-(4-butyl-2-methylphenyl)formamidine], a selective inhibitor of CYP4A. J Pharmacol Exp Ther 315:526
10. Alexanian A, Rufanova VA, Miller B, Flasch A, Roman RJSorokin A (2009) Down-regulation of 20-HETE synthesis and signaling inhibits renal adenocarcinoma cell proliferation and tumor growth. Anticancer Res 29:3819
11. Guo AM, Sheng J, Scicli GM, Arbab AS, Lehman NL, Edwards PA, Falck JR, Roman RJScicli AG (2008) Expression of CYP4A1 in U251 human glioma cell induces hyperproliferative phenotype in vitro and rapidly growing tumors in vivo. J Pharmacol Exp Ther 327:10
12. Guo AM, Arbab AS, Falck JR, Chen P, Edwards PA, Roman RJScicli AG (2007) Activation of vascular endothelial growth factor through reactive oxygen species mediates 20-hydroxyeicosatetraenoic acid-induced endothelial cell proliferation. J Pharmacol Exp Ther 321:18
13. Yamane M, Abe A (2000) Omega-hydroxylation activity toward leukotriene B(4) and polyunsaturated fatty acids in the human hepatoblastoma cell line, HepG2, and human lung adenocarcinoma cell line, A549. J Biochem 128:827
14. Kadota K, Huang CL, Liu D, Ueno M, Kushida Y, Haba RYokomise H (2008) The clinical significance of lymphangiogenesis and angiogenesis in non-small cell lung cancer patients. Eur J Cancer 44:1057
15. Rasheed SA, Efferth T, Asangani IA, Allgayer H (2010) First evidence that the anti-malarial drug Artesunate inhibits invasion and in vivo metastasis in lung cancer by targeting essential extracellular proteases. Int J Cancer 127:1475
16. Shah SA, Spinale FG, Ikonomidis JS, Stroud RE, Chang EI, Reed CE (2010) Differential matrix metalloproteinase levels in adenocarcinoma and squamous cell carcinoma of the lung. J Thorac Cardiovasc Surg 139:984
17. Iniesta P, Moran A, De Juan C, Gomez A, Hernando F, Garcia-Aranda C, Frias C, Diaz-Lopez A, Rodriguez-Jimenez FJ, Balibrea JLBenito M (2007) Biological and clinical significance of MMP-2, MMP-9, TIMP-1 and TIMP-2 in non-small cell lung cancer. Oncol Rep 17:217
18. Safranek J, Pesta M, Holubec L, Kulda V, Dreslerova J, Vrzalova J, Topolcan O, Pesek M, Finek J, Treska V (2009) Expression of MMP-7, MMP-9, TIMP-1 and TIMP-2 mRNA in lung tissue of patients with non-small cell lung cancer (NSCLC) and benign pulmonary disease. Anticancer Res 29:2513
19. Hicklin DJ, Ellis LM (2005) Role of the vascular endothelial growth factor pathway in tumor growth and angiogenesis. J Clin Oncol 23:1011
20. Lee S, Jilani SM, Nikolova GV, Carpizo D, Iruela-Arispe ML (2005) Processing of VEGF-A by matrix metalloproteinases regulates bioavailability and vascular patterning in tumors. J Cell Biol 169:681
21. Houck KA, Leung DW, Rowland AM, Winer J, Ferrara N (1992) Dual regulation of vascular endothelial growth factor bioavailability by genetic and proteolytic mechanisms. J Biol Chem 267:26031
22. Ortega N, L'Faqihi FE, Plouet J (1998) Control of vascular endothelial growth factor angiogenic activity by the extracellular matrix. Biol Cell 90:381
23. Deryugina EI, Quigley JP (2006) Matrix metalloproteinases and tumor metastasis. Cancer Metastasis Rev 25:9
24. Carmeliet P, Jain RK (2000) Angiogenesis in cancer and other diseases. Nature 407:249
25. Wang DS, Miller R, Shaw R, Shaw G (1996) The Pleckstrin homology domain of human βI$\sum$II spectrin is targeted to the plasma membrane in vivo. Biochem Biophys Res Commun 225:420
26. Cai KX, Tse LY, Leung C, Tam PK, Xu R, Sham MH (2008) Suppression of lung tumor growth and metastasis in mice by adeno-associated virus-mediated expression of vasostatin. Clin Cancer Res 14:939
27. Doki Y, Murakami K, Yamaura T, Sugiyama S, Misaki T, Saiki I (1999) Mediastinal lymph node metastasis model by orthotopic intrapulmonary implantation of Lewis lung carcinoma cells in mice. Br J Cancer 79:1121
28. Lv X, Wan J, Yang J, Cheng H, Li Y, Ao Y, Peng R (2008) Cytochrome P450 omega- hydroxylase inhibition reduces cardiomyocyte apoptosis via activation of ERK1/2 signaling in rat myocardial ischemia-reperfusion. Eur J Pharmacol 596:118

29. Duffy MJ, Duggan C (2004) The urokinase plasminogen activator system: a rich source of tumour markers for the individualised management of patients with cancer. Clin Biochem 37:541
30. Rofstad EK, Mathiesen B, Kindem K, Galappathi K (2006) Acidic extracellular pH promotes experimental metastasis of human melanoma cells in athymic nude mice. Cancer Res 66:6699
31. Fidler IJ, Ellis LM (1994) The implications of angiogenesis for the biology and therapy of cancer metastasis. Cell 79:185
32. Lamoreaux WJ, Fitzgerald ME, Reiner A, Hasty KA, Charles ST (1998) Vascular endothelial growth factor increases release of gelatinase A and decreases release of tissue inhibitor of metalloproteinases by microvascular endothelial cells in vitro. Microvasc Res 55:29
33. Kaplan RN, Psaila B, Lyden D (2007) Niche-to-niche migration of bone-marrow-derived cells. Trends Mol Med 13:72
34. Guo M, Roman RJ, Fenstermacher JD, Brown SL, Falck JR, Arbab AS, Edwards PA, Scicli AG (2006) 9L gliosarcoma cell proliferation and tumor growth in rats are suppressed by N-hydroxy-N'-(4-butyl-2-methylphenol) formamidine (HET0016), a selective inhibitor of CYP4A. J Pharmacol Exp Ther 317:97
35. Hukkanen J, Lassila A, Päivärinta K, Valanne S, Sarpo S, Hakkola J, Pelkonen O, Raunio H (2000) Induction and regulation of xenobiotic-metabolizing cytochrome P450 s in the human A549 lung adenocarcinoma cell line. Am J Respir Cell Mol Biol 22:360
36. Jiang BH, Liu LZ (2008) AKT signaling in regulating angiogenesis. Curr Cancer Drug Targets 8:19
37. Qiao M, Sheng S, Pardee AB (2008) Metastasis and AKT activation. Cell Cycle 7:2991
38. Reddy KB, Nabha SM, Atanaskova N (2003) Role of MAP kinase in tumor progression and invasion. Cancer Metastasis Rev 22:395
39. Dhanasekaran A, Bodiga S, Gruenloh S, Gao Y, Dunn L, Falck JR, Buonaccorsi JN, Medhora M, Jacobs ER (2009) 20-HETE increases survival and decreases apoptosis in pulmonary arteries and pulmonary artery endothelial cells. Am J Physiol Heart Circ Physiol 296:H777